



An analysis of lncRNA-miRNA-mRNA networks to investigate the effects of HDAC4 inhibition on skeletal muscle atrophy caused by peripheral nerve injury

Yuming Gu^{1#}, Yinghao Lin^{1#}, Ming Li^{2#}, Chenyu Zong¹, Hualin Sun³, Yuntian Shen³, Jianwei Zhu¹

¹Department of Orthopedics, Affiliated Hospital of Nantong University, Nantong, China; ²Department of Laboratory Medicine, Binhai County People's Hospital affiliated to Kangda College of Nanjing Medical University, Yancheng, China; ³Key Laboratory of Neuroregeneration of Jiangsu and Ministry of Education, Co-Innovation Center of Neuroregeneration, NMPA Key Laboratory for Research and Evaluation of Tissue Engineering Technology Products, Jiangsu Clinical Medicine Center of Tissue Engineering and Nerve Injury Repair, Nantong University, Nantong, China

Contributions: (I) Conception and design: J Zhu, Y Shen; (II) Administrative support: J Zhu, H Sun, Y Shen; (III) Provision of study materials or patients: Y Gu, Y Lin, M Li, C Zong, H Sun, Y Shen; (IV) Collection and assembly of data: Y Gu, Y Lin, M Li, Y Shen; (V) Data analysis and interpretation: Y Gu, J Zhu, Y Shen, H Sun; (VI) Manuscript writing: All authors; (VII) Final approval of manuscript: All authors.

[#]These authors contributed equally to this work.

Correspondence to: Professor Jianwei Zhu. Affiliated Hospital of Nantong University, 20 Xisi Road, Nantong 226001, China. Email: zhujianwei_nt@163.com; Yuntian Shen. Key Laboratory of Neuroregeneration of Jiangsu and Ministry of Education, Nantong University, 19 Qixiu Road, Nantong 226001, China. Email: syt517@ntu.edu.cn.

Background: Muscle atrophy caused by peripheral nerve injury is a common clinical disease, with no effective treatments currently available. Our previous studies have found that denervation-induced muscle atrophy can be alleviated by inhibiting histone deacetylase 4 (HDAC4). An increasing amount of evidence shows that microRNA (miRNA) and long noncoding RNA (lncRNA) are involved in the occurrence of muscle atrophy. This study aimed to find the mechanism by which HDAC4 regulates denervation-induced muscle atrophy based on lncRNA-associated competing endogenous RNA (ceRNA) networks.

Methods: We analyzed the influence of short hairpin RNA (shRNA) knockdown of HDAC4 on lncRNAs and miRNAs after denervated muscle atrophy using RNA sequencing. A Pearson's correlation heat map and principal component analysis were employed to analyze differentially expressed miRNAs and lncRNAs. Gene Ontology and Kyoto Encyclopedia of Genes and Genomes enrichment analyses of target genes were conducted. The ceRNA network of lncRNA-miRNA-mRNA was constructed, and the core regulatory molecules in the ceRNA network were analyzed.

Results: We found 32 miRNAs and 111 lncRNAs related to denervated muscle atrophy regulated by HDAC4. Moreover, 15 downregulated lncRNAs, 14 upregulated miRNAs, and 61 downregulated mRNAs constituted a ceRNA regulatory network, participating in the biological processes including response to denervation involved in regulation of muscle adaptation, along with the signaling pathways including autophagy, FoxO signaling pathways, and Jak-STAT signaling pathways. Additionally, 6 upregulated lncRNAs, 8 downregulated miRNAs, and 66 upregulated mRNAs constituted another ceRNA regulatory network, which was mainly involved in cell cycle-related biological processes and pathways. Finally, 3 lncRNAs, 4 miRNAs, and 12 mRNAs constituted a ceRNA sub-network, and XR_377582.2 and ENSMUST00000143649 were considered to be the key lncRNAs.

Conclusions: In the ceRNA network, all nodes are directly or indirectly involved in the process by which HDAC4 regulates skeletal muscle atrophy caused by peripheral nerve injury. XR_377582.2 and ENSMUST00000143649 may be the key lncRNAs related to HDAC4 involved in the regulation of muscle atrophy.

Keywords: Denervation; muscle atrophy; competing endogenous RNA (ceRNA); histone deacetylase 4 (HDAC4); transcriptome sequencing

Submitted Dec 03, 2021. Accepted for publication Jan 30, 2022.

doi: 10.21037/atm-21-6512

View this article at: <https://dx.doi.org/10.21037/atm-21-6512>

Introduction

Skeletal muscle is the largest tissue in the human body, and its structural integrity and functional maintenance are all under the control of the nervous system. The treatment of peripheral nerve injury caused by traumatic or chemical insult, still remains a challenge to be resolved. Following peripheral nerve injury, nerve regeneration occurs at a very slow rate. The target organ loses the trophic support of the nerve, triggering a series of reactions, such as oxidative stress, inflammation, mitochondrial autophagy, and catabolism. These series of reactions can cause skeletal muscle atrophy, which can be extended and aggravated over time (1,2). In severe cases, patients often experience irreversible atrophy, and atrophic muscle may be unable to be innervated by regenerated nerves, eventually resulting in a loss of function (3). Therefore, it is crucial to find the trigger factors that initiate skeletal muscle atrophy in the early stage of denervation and to intervene to delay the process of skeletal muscle atrophy after nerve injury.

We used a microarray to analyze the changes in gene expression levels of the tibialis anterior in rats at 15 minutes to 28 days after denervation. Our findings led us to propose the following 4 stages for the transcriptional regulation of denervation-induced skeletal muscle atrophy: oxidative stress stage (0.25–12 hours post-nerve injury), inflammation stage (24 hours post-nerve injury), atrophy stage (3–7 days post-nerve injury), and atrophic fibrosis stage (14–28 days post-nerve injury) (1). We further analyzed microarray data and screened out hub gene-histone deacetylase 4 (HDAC4) (1). HDAC4 is a class IIa histone deacetylase, belonging to an important epigenetic modifying enzyme family. HDAC4 affects the binding of transcription factors to DNA by transforming the status of histone acetylation and/or deacetylation. Studies have shown the expression of HDAC4 to be increased in a variety of muscle atrophy models, and HDAC4 can cause the deacetylation of MyHC subtypes, PGC-1 α , and Hsc70 (4–6). In our recent work, we found that HDAC4 inhibition can inhibit proteolysis and mitochondrial autophagy caused by denervation and reversed denervation-induced tibialis anterior muscle atrophy (7).

Noncoding RNAs (ncRNAs), including microRNA (miRNAs) and long noncoding RNA (lncRNAs), have a

regulatory role in skeletal muscle production and atrophy (8,9). miRNAs are a type of noncoding RNA with a length of 20–25 nucleotides, and they enact their biological activities by binding to the 3'-untranslated region (3'-UTR) of target gene messenger RNAs (mRNAs). Studies have shown that various miRNAs, such as miR-23a and miR-1, can bind to the E3 ubiquitin ligase MuRF1 and MAFbx of the ubiquitin protease system to inhibit their translation activation, regulate muscle atrophy thereby (10,11). Our previous studies also found that miR-125b-5p and miR-351 can alleviate muscle atrophy by targeting *TRAF6* (12,13). lncRNAs are a type of regulatory RNAs with a length ranging from 200 bp to >100 kb, and they have an extremely abundant number of miRNA binding sites. According to competing endogenous RNA (ceRNA) theory, lncRNAs, acting as miRNA sponge by miRNA response elements (MREs), form a ceRNA network to modulate mRNA expression (14). For example, *LINC-MD1* can regulate the expression of transcription factors, MAML1 and MEF2C, which activate late-differentiated muscle genes by binding to miR-133 and miR-135 (15). *LNCIRS1* can regulate the expression of IRS1 via sponging the miR-15 family, thereby controlling skeletal muscle myogenesis and atrophy (16). Although a few lncRNAs have been functionally annotated, the role of most lncRNAs in myogenesis and atrophy is still unclear. Thus, the purpose of this study was to clarify the regulatory mechanism by which HDAC4 regulates skeletal muscle atrophy based on ceRNA theory.

In this study, we processed high-throughput sequencing data. First, we analyzed the miRNAs related to HDAC4 regulation of muscle atrophy, based on which we constructed the lncRNA-miRNA-mRNA network and performed functional enrichment analysis and annotations. We further explored the importance of lncRNAs in muscle atrophy. Finally, we found the core regulatory RNA molecules in the ceRNA network through analysis. Our findings provide important clues to exploring the mechanism by which HDAC4 regulates muscle atrophy and enriches the potential functions of lncRNA-based ceRNA networks in the process of HDAC4 regulating muscle atrophy. Studying the potential mechanism of HDAC4 in the process of muscle atrophy provides an important experimental basis for discovering new targets

for the prevention and treatment of denervation-induced skeletal muscle atrophy. We present the following article in accordance with the ARRIVE (Animal Research: Reporting of In Vivo Experiments) reporting checklist (available at <https://atm.amegroups.com/article/view/10.21037/atm-21-6512/rc>).

Methods

Animal experiment

Adult male 8 to 12-week-old Institute of Cancer Research (ICR) mice weighing 25 ± 2 g, were provided by the Experimental Animal Center of Nantong University. All animals were caged at 22 °C in a 12-hour light-dark cycle environment and moved freely with free access to water and food. The ICR mice were randomly divided into 3 groups ($n=3$ per group). The left tibialis anterior of the mice was exposed under anesthesia, and lentivirus ($25 \mu\text{L}$, 1×10^8 TU) expressing HDAC4-shRNA (Hi + Den) was injected into the tibialis anterior muscles as previously described (7). An identical amount of empty vector virus was injected in the control group (Ctr) and denervation group (Den). The lentivirus vector for shRNA was GV298, and the component sequence was U6-MCS-Ubiquitin-Cherry-IRES-puromycin. After 3 days, the left sciatic nerve of the mice in the HDAC4 inhibition and denervation groups was cut, and the proximal end of the sciatic nerve was reflexed and sutured under the skin to produce a 10-mm defect model (17,18). In the control group, the sciatic nerve was only exposed but not dissected. Mice were euthanized under anesthesia on day 7, and the tibialis anterior was dissected and frozen on liquid nitrogen. Experiments were performed under a project license (No. 20180305-004) granted by the Jiangsu Laboratory Animal Management Committee, in compliance with Nantong University guidelines for the care and use of animals.

Transcriptome sequencing

Library construction and sequencing were implemented as previously described (19). In short, total RNA was extracted using the mirVana miRNA Isolation Kit (Ambion, Austin, TX, USA) according to the manufacturer's protocol. Quantitation of total RNA was carried out using the Nanodrop 2000 (Thermo Fisher Scientific Inc., Waltham, MA, USA). RNA integrity was assessed using Agilent 2100 Bioanalyzer (Agilent Technology, Santa Clara, CA,

USA). The total RNA ($1 \mu\text{g}$) of each sample was used for the small RNA library construction using TruSeq Small RNA Sample Prep Kits (Illumina, San Diego, CA, USA) following the manufacturer's instructions, and $1 \mu\text{g}$ of total RNA of each sample was used for lncRNA library construction using TruSeq Stranded Total RNA with Ribo-Zero Gold (Illumina) according to the manufacturer's instructions. Briefly, total RNA was ligated to adapters at each end. Then, the adapter-ligated RNA was reverse transcribed to circular DNA (cDNA), and polymerase chain reaction (PCR) amplification was performed. The PCR products ranging from 140–160 bp were isolated and purified as small RNA libraries. Library quality was assessed using the Agilent Bioanalyzer 2100 system (Agilent Technologies) using DNA High Sensitivity Chips. The libraries were finally sequenced using the Illumina HiSeq X Ten platform, and 150-bp paired-end reads were generated. The miRNA and lncRNA expression profiles are available on ArrayExpress (<https://ftp.ebi.ac.uk/pub/databases/microarray/data>), and the accession numbers are E-MTAB-11362 and E-MTAB-11361, respectively.

Expression analysis

The original data generated by sequencing were filtered out to obtain high-quality clean reads. Clean data were obtained by removing reads containing adapter and poly-N or low-quality reads from raw data. Candidate lncRNA transcripts were screened out using Stringtie2 software (1.3.3b version, John Hopkins University, Baltimore, MD, USA) and Cuffcompare software (2.2.1 version, The University of Maryland, Baltimore, MD, USA), and transcripts with coding potential were then removed to obtain the predicted sequence of lncRNA. The sequencing reads of each sample were aligned to the combined sequence of mRNA transcript sequence, known lncRNA sequence, and lncRNA-predicted sequence using bowtie2 (2.2.9 version, John Hopkins University) (20), and eXpress software (version 1.5.1, Express Software Production, East Granby, CT, United States) was used for gene quantification to obtain the FPKM (fragments per kilobase per million) value and counts. The counts were standardized through the estimateSizeFactors function of the DESeq R package (1.18.0 version, Fred Hutchinson Cancer Research Center, Seattle, WA, USA), and the P and fold change values for difference comparison were calculated using the nbinomTest function. lncRNAs (fold change < 1.5 or > 1.5 and $P < 0.05$) were sorted out.

The original reads obtained by small RNA sequencing

were first removed of adaptor sequences and filtered using Cutadapt (1.14 version, National Bioinformatics Infrastructure, Uppsala, Sweden). High-quality clean reads were then obtained following filtration using fastx_toolkit (0.0.13 version, Cancer Research UK Cambridge Institute, Cambridge, UK) and National Institute of Plant Genome Research Toolkit (2.3.2 version, National Institute of Plant Genome Research, New Delhi, India), which were used for subsequent analysis. Filtered data were compared using Blastn (2.2.26 version, National Center for Biotechnology, Bethesda, MD, USA) and RepeatMasker (4.0.9 version, <http://www.repeatmasker.org>) software. A new miRNA prediction using Mirdeep2 (2.0.0.8 version, Max Delbrueck Center for Molecular Medicine, Berlin, Germany) was conducted in the unannotated small RNA sequences, and the secondary structure of the newly predicted miRNA was predicted using RNAfold (2.4.9 version, University of Vienna, Vienna, Austria). Based on the known mature miRNA and newly predicted miRNA, miRNA expression was statistically quantified as transcripts per million (TPM). TPM is equal to the number of reads mapped to each miRNA/the total number of mapped reads $\times 10^6$. TPM indicates that counts come from a transcript per million reads mapped, and the total number of paired-end reads mapped is used to normalize the expression level. The Audic_Claverie formula was used to calculate P value, and the miRNAs with fold change ≤ -1.5 or > 1.5 and $P < 0.05$ were selected. The mRNA expression profile was analyzed based on our published RNA sequence data, which is available on ArrayExpress (accession no. E-MTAB-11361) (7). Differentially expressed mRNAs were defined as mRNAs with $P < 0.05$ and a fold change ≤ -1.5 or > 1.5 .

CeRNA network analysis

Based on the expression of different mRNAs, miRNAs, and lncRNAs, Pearson's correlation coefficients and P values were calculated for miRNA-target pairs. Pearson correlation coefficients ≥ 0.8 or ≤ -0.8 with $P < 0.05$ were considered statistically significant. Among these negatively correlated miRNA-lncRNAs, candidate mRNAs and lncRNAs regulated by the miRNAs were predicted using miRanda v3.3a (<http://www.microrna.org/microrna/>). The threshold parameter was set as described previously: $S \geq 150$, $\Delta G \leq -30$ kcal/mol and strict 5' seed pairing (21). Subsequently, shared pairs of miRNA-mRNA and miRNA-lncRNA were used to predict ceRNA scores using MuTaME (22) according to the following formula: $ceRNA_score = MRE_for_share_miRNA/MRE_for_lncRNA_miRNA$; the related P values were calculated using Benjamini and Hochberg's approach for controlling the false discovery rate (23). The positively correlated pairs of lncRNA-mRNA based on the ceRNA score principle were then considered as the true ceRNAs.

miRNA/MRE_for_lncRNA_miRNA; the related P values were calculated using Benjamini and Hochberg's approach for controlling the false discovery rate (23). The positively correlated pairs of lncRNA-mRNA based on the ceRNA score principle were then considered as the true ceRNAs.

Construction of lncRNA-associated ceRNA networks

Based on the above sequencing data analysis, Cytoscape v. 3.8.2 software (Institute for Systems Biology, Seattle, WA, USA) was used to construct a lncRNA-related ceRNA network. The subnetwork containing the hub gene was identified using a Cytoscape plugin, MCODE.

Functional annotation

The Kyoto Encyclopedia of Genes and Genomes (KEGG) pathway was used to analyze the significance of the target genes of differentially expressed miRNA with the mirPath v.3 online tool of DIANA TOOLS (<http://snf-515788.vm.okeanos.grnet.gr/index.php?r=mirpath>). Gene Ontology (GO) and KEGG pathway analyses were completed online for mRNAs in the ceRNA network (<https://david.ncifcrf.gov/summary.jsp>). KEGG or GO terms with $P < 0.05$ were considered to be significantly enriched.

Statistical analysis

When RNA-seq data are used to compare and analyze whether there is differential expression of the same gene in 2 samples, 2 criteria can be selected: one is fold change, which is the change multiple of the same gene expression level in two samples; the other is the P value. The default screening condition was $P < 0.05$, and the difference multiple was more than 1.5.

Results

Effect of HDAC4 inhibition on miRNA expression changes of skeletal muscle atrophy caused by peripheral nerve injury

We performed a miRNA-seq analysis to determine the effect of HDAC4 inhibition on miRNAs in mice with denervation-induced skeletal muscle atrophy. There were a total of 1,148 annotated miRNAs and 841 newly predicted miRNAs in all the samples. Hierarchical clustering showed that miRNAs were well distinguished in the control group (Ctr), denervation group (Den), and HDAC4 inhibition

group (Hi + Den), and all samples were correctly classified (Figure 1A). Principal component analysis (PCA) results indicated there were different expression characteristics of miRNAs in samples from different groups (Figure 1B). Compared with the Ctr group, there were 155 downregulated miRNAs and 97 upregulated miRNAs in the Den group; compared with the Den group, there were 123 upregulated miRNAs and 73 downregulated miRNAs in the Hi + Den group (Figure 1C). The intersection of downregulated miRNAs after denervation and upregulated miRNAs after HDAC4 inhibition was identified, and these intersected miRNAs were then referred to as upregulated miRNAs, including mmu-miR-6691-5p, mmu-miR-3095-3p, mmu-miR-449a-5p, mmu-miR-146a-5p, mmu-miR-592-5p, mmu-miR-298-5p, mmu-miR-376b-3p, mmu-miR-296-3p, mmu-miR-362-3p, mmu-miR-296-5p, mmu-miR-362-5p, mmu-miR-181c-3p, mmu-miR-500-3p, mmu-miR-501-3p, mmu-miR-181a-1-3p, and mmu-miR-335-3p (Table 1). The intersection of upregulated miRNAs after denervation and downregulated miRNAs after HDAC4 inhibition was identified, and these intersected miRNAs were then referred to as downregulated miRNAs, including novel159_mature, mmu-miR-9-5p, mmu-miR-9-3p, novel489_mature, novel630_mature, novel6_mature, mmu-miR-128-3p, mmu-miR-671-3p, novel162_mature>novel498_mature, mmu-miR-27a-5p, novel374_mature>novel461_mature, mmu-miR-30a-5p, mmu-miR-30c-2-3p, mmu-miR-5099, mmu-miR-149-5p, and novel356_mature (Table 1). KEGG analysis of target genes was conducted using the mirPath online tool to determine their related signal pathways. KEGG analysis results showed that the upregulated miRNAs were mainly involved in the regulation of pathways in cancer, thyroid hormone signaling pathway, adherens junction, FoxO signaling pathway, ubiquitin-mediated proteolysis, Wnt signaling pathway, and protein processing in endoplasmic reticulum pathways (Figure 1D), while the downregulated miRNAs were mainly involved in the regulation of fatty acid biosynthesis, protein processing in endoplasmic reticulum, axon guidance, glycosaminoglycan biosynthesis-chondroitin sulfate/dermatan sulfate, and neurotrophin signaling pathway processes (Figure 1E).

Effect of HDAC4 inhibition on lncRNA expression changes of denervation-induced skeletal muscle atrophy

Subsequently, we conducted a lncRNA-Seq analysis, and there were 34,458 lncRNAs detected in total, from which

678 newly predicted lncRNAs were identified. Hierarchical clustering analysis showed that the lncRNAs were well distinguished in the Ctr, Den, and Hi + Den groups, and all samples were correctly classified (Figure 2A). The PCA results showed the different expression characteristics of lncRNAs in samples from different groups (Figure 2B). Compared with the Ctr group, there were 377 downregulated lncRNAs and 454 upregulated lncRNAs in the Den group. Compared with the denervation group, there were 304 upregulated lncRNAs and 178 downregulated lncRNAs in Hi + Den group (Figure 2C). Among the differentially expressed lncRNAs, 20% were located in the exons of protein-coding genes, 23% were located in the introns, and 26% and 18% were located in the upstream and downstream of the intragenic region, respectively (Figure 2D). Furthermore, when the chromosome distribution and sequence length distribution of the lncRNAs were analyzed, there were more lncRNAs located on chromosome 1 (Figure 2E,2F).

DE lncRNAs, miRNAs, and mRNAs formed gene-gene networks by mutual interaction

The upregulated lncRNAs were defined as the intersection of downregulated lncRNAs after denervation and upregulated lncRNA after HDAC4 inhibition. The downregulated lncRNAs were defined as the intersection of upregulated lncRNAs after denervation and downregulated lncRNA after HDAC4 inhibition. The final sample included 27 upregulated lncRNAs and 84 downregulated lncRNAs (Table 2). To better understand the regulatory role of lncRNA and miRNA in HDAC4 regulation of muscle atrophy, we constructed a lncRNA-miRNA-mRNA ceRNA network to further clarify the interaction of specific differential lncRNAs, miRNAs, and mRNAs. A ceRNA regulatory network was composed of 15 downregulated lncRNAs, 14 upregulated miRNAs, and 61 downregulated mRNAs. In this network, E3 ubiquitin ligase genes, Fbxo32 and Trim63, were closely related to muscle atrophy (Figure 3A). In addition, 6 upregulated lncRNAs, 8 downregulated miRNAs, and 66 upregulated mRNAs constituted another ceRNA regulatory network (Figure 3B).

GO and KEGG pathway analyses

GO analysis and KEGG pathway analysis showed that after inhibition with HDAC4, in the ceRNA network that downregulated lncRNAs belonged to, the mRNAs participated in the biological processes, such as response to

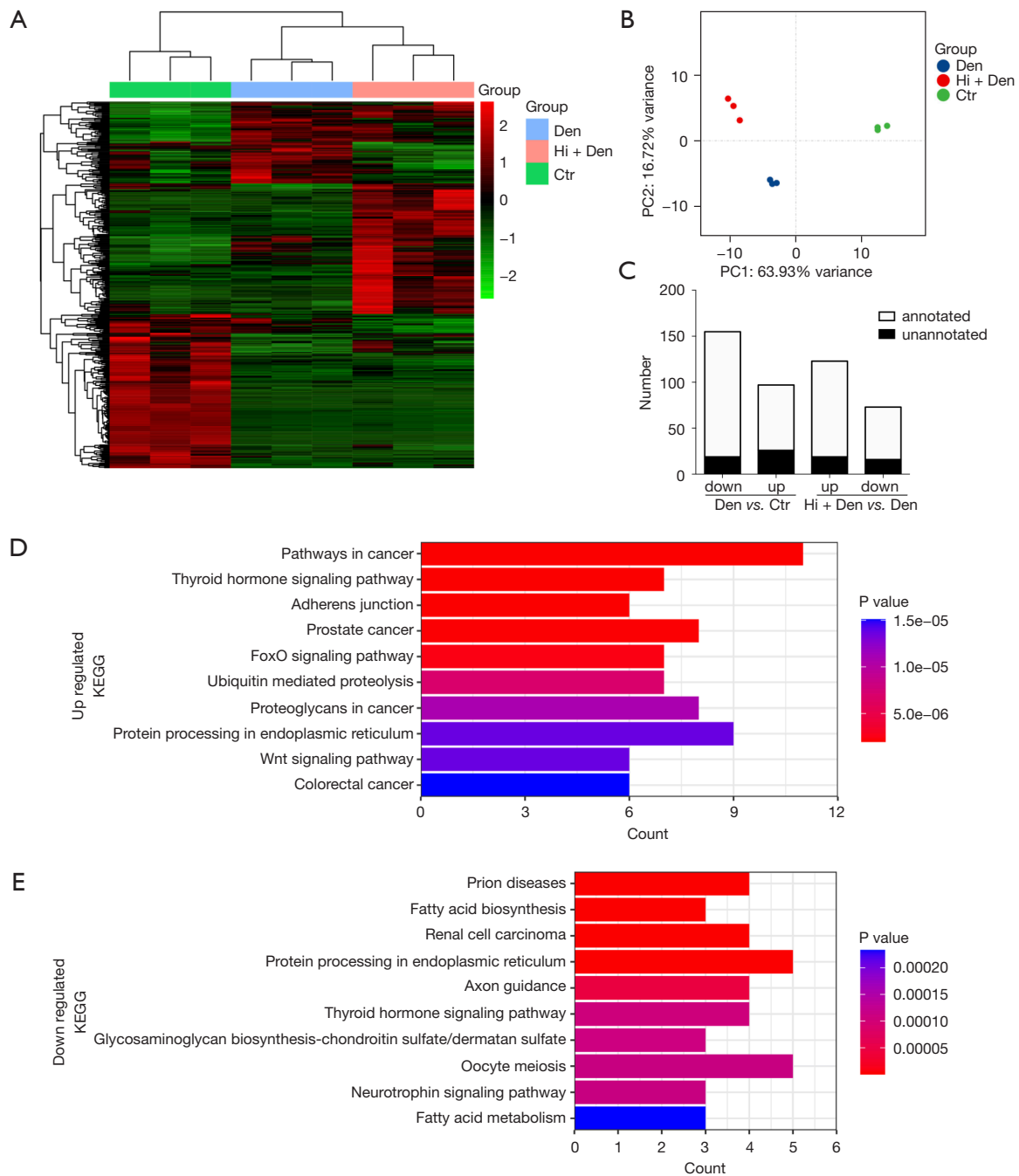


Figure 1 Changes in the expression of microRNA (miRNAs) after skeletal muscle atrophy. (A) Heat map of differentially expressed miRNAs in the histone deacetylase 4 (HDAC4) inhibition group (Hi + Den), denervation group (Den), and control group (Ctr) 7 days after the operation; clustering of all the differentially expressed miRNA ($P < 0.05$; fold change < -1.5 or > 1.5). The standardized expression level from green to red represents the expression level from low to high; $n = 3$. (B) Principal component analysis (PCA) of differentially expressed miRNA; the PCA was performed with normalized counts. (C) The number of upregulated and downregulated miRNAs after different treatments. (D) Kyoto Encyclopedia of Genes and Genomes (KEGG) analysis of upregulated miRNAs (downregulated miRNA after denervation and upregulated miRNA after HDAC4 inhibition), which were further screened. (E) KEGG analysis of downregulated miRNAs (upregulated miRNA after denervation and downregulated miRNA after HDAC4 inhibition), which were screened further. The x-axis indicates the number of genes, and the y-axis indicates the KEGG term. The color bar shows the P value.

Table 1 HDAC4-regulated atrophy-related microRNA

miRNA_id	Den vs. Ctr		Hi + Den vs. Den		Hi + Den vs. Ctr	
	log2(FC)	P val	log2(FC)	P val	log2(FC)	P val
Upregulated						
mmu-miR-669l-5p	-2.32	0.0474	3.68	<0.0001	1.40	0.0315
mmu-miR-3095-3p	-2.71	0.0012	2.89	0.0006	0.22	0.8114
mmu-miR-449a-5p	-1.11	0.0467	2.89	0.0023	1.83	0.0220
mmu-miR-146a-5p	-0.69	<0.0001	2.84	<0.0001	2.19	<0.0001
mmu-miR-592-5p	-0.80	0.0108	2.27	<0.0001	1.51	<0.0001
mmu-miR-298-5p	-3.14	<0.0001	2.04	<0.0001	-1.07	0.0002
mmu-miR-376b-3p	-3.16	<0.0001	1.81	0.0019	-1.31	0.0016
mmu-miR-296-3p	-2.56	<0.0001	1.59	0.0030	-0.94	0.0083
mmu-miR-362-3p	-0.72	0.0009	1.38	<0.0001	0.70	0.0041
mmu-miR-296-5p	-2.50	<0.0001	1.16	0.0002	-1.30	0.0002
mmu-miR-362-5p	-1.01	<0.0001	1.07	<0.0001	0.10	0.6494
mmu-miR-181c-3p	-1.76	<0.0001	1.01	0.0020	-0.72	0.0162
mmu-miR-500-3p	-0.89	0.0003	0.97	0.0002	0.11	0.7105
mmu-miR-501-3p	-0.85	<0.0001	0.85	<0.0001	0.04	0.8429
mmu-miR-181a-1-3p	-0.88	0.0001	0.78	0.0016	-0.07	0.7900
mmu-miR-335-3p	-2.48	<0.0001	0.77	0.0028	-1.67	<0.0001
Downregulated						
novel159_mature	2.12	0.0284	-5.21	0.0007	-3.07	0.1407
mmu-miR-9-5p	2.89	<0.0001	-3.05	<0.0001	-0.13	0.5589
mmu-miR-9-3p	1.72	0.0143	-2.67	0.0010	-0.91	0.0638
novel489_mature	1.38	0.0438	-1.33	0.0328	0.07	1.0000
novel630_mature	1.03	0.0121	-1.33	0.0019	-0.26	0.6446
novel6_mature	1.64	<0.0001	-1.19	<0.0001	0.49	0.1288
mmu-miR-128-3p	0.64	0.0003	-1.10	<0.0001	-0.41	0.0237
mmu-miR-671-3p	1.19	<0.0001	-1.06	0.0001	0.17	0.5866
novel162_mature>novel498_mature	2.63	<0.0001	-1.01	0.0202	1.67	0.0086
mmu-miR-27a-5p	1.75	<0.0001	-0.88	0.0004	0.92	0.0019
novel374_mature>novel461_mature	0.93	0.0218	-0.85	0.0402	0.11	0.8516
mmu-miR-30a-5p	0.92	<0.0001	-0.83	0.0001	0.12	0.6070
mmu-miR-30c-2-3p	0.63	0.0051	-0.80	<0.0001	-0.13	0.4555
mmu-miR-5099	1.55	<0.0001	-0.70	0.0035	0.89	0.0014
mmu-miR-149-5p	0.80	<0.0001	-0.69	0.0003	0.14	0.4986
novel356_mature	0.63	0.0484	-0.60	0.0360	0.07	0.8608

FC, fold change; Ctr, control group; Den, denervation group; Hi + Den, HDAC4 inhibition group; miRNA, microRNA.

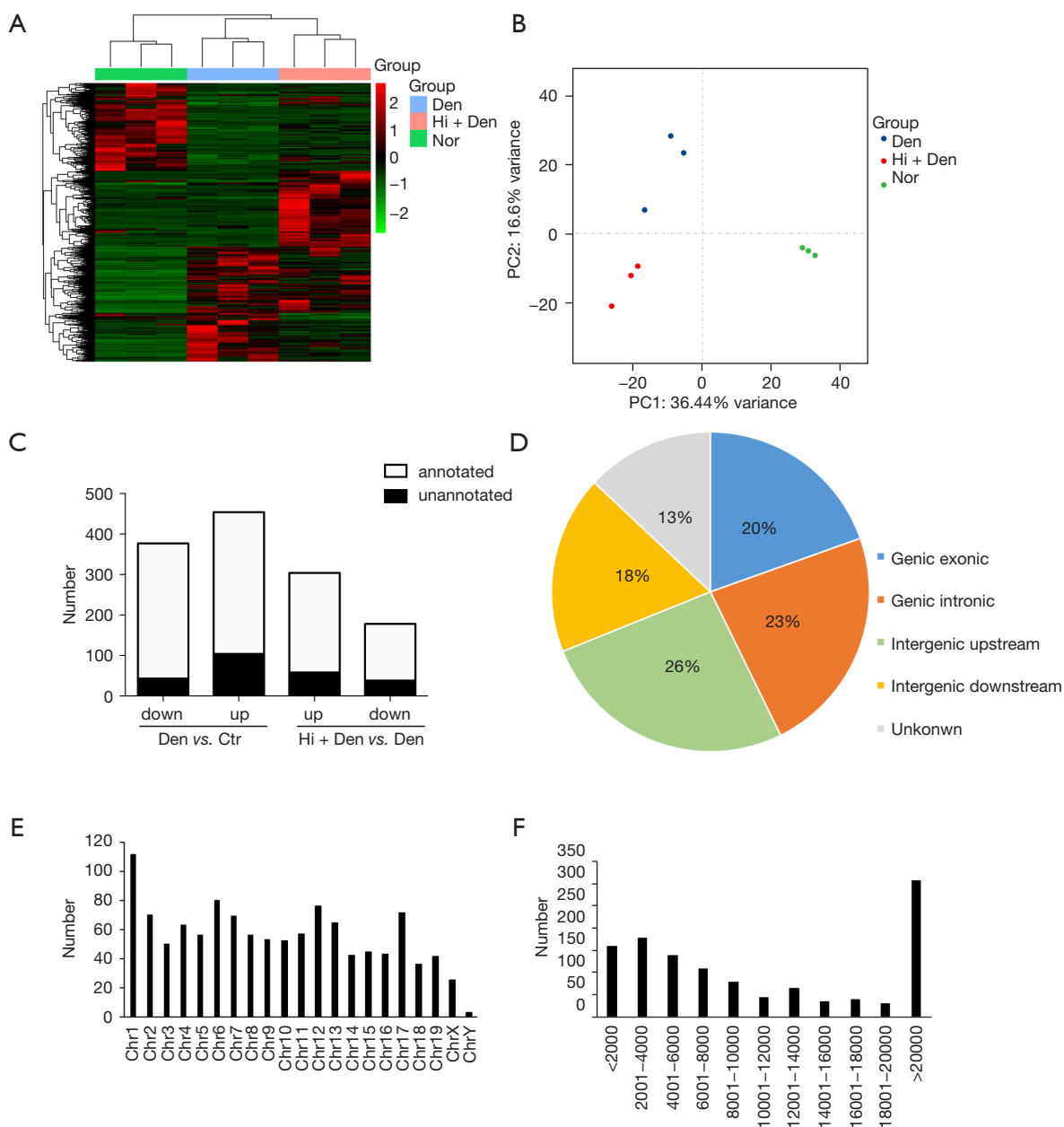


Figure 2 Changes in the expression of long noncoding RNA (lncRNAs) in skeletal muscle atrophy regulated by histone deacetylase 4 (HDAC4). (A) Heat map of differentially expressed lncRNA in the HDAC4 inhibition group (Hi + Den), denervation group (Den), and control group (Ctr) 7 days after the operation. Clustering of all the differentially expressed lncRNA ($P < 0.05$; fold change < -1.5 or > 1.5). The standardized expression level from green to red represents expression level from low to high; $n = 3$. (B) Principal component analysis (PCA) of differentially expressed lncRNAs. The PCA was performed with normalized counts. (C) Number of upregulated and downregulated lncRNAs after different treatments. (D) Subgroup analysis of differentially expressed lncRNAs based on gene location and association with adjacent protein-coding genes. (E) Chromosome distribution of the differentially expressed lncRNAs. (F) Sequence length distribution of the differentially expressed lncRNAs.

Table 2 HDAC4-regulated atrophy-related long noncoding RNAs

lncRNA_id	Den vs. Ctr		Hi + Den vs. Den		Hi + Den vs. Ctr	
	log2(FC)	P val	log2(FC)	P val	log2(FC)	P val
Downregulated						
ENSMUST00000230832	5.29	0.0120	-Inf	0.0021	-Inf	0.9669
TCONS_00009025	3.64	0.0292	-Inf	0.0003	-Inf	0.6232
TCONS_00026499	Inf	0.0094	-Inf	0.0057	0.00	1.0000
XR_001784025.1	Inf	0.0211	-Inf	0.0062	0.00	1.0000
XR_378108.2	Inf	0.0307	-Inf	0.0188	0.00	1.0000
XR_382507.3	Inf	0.0268	-Inf	0.0149	0.00	1.0000
XR_390555.3	4.50	0.0176	-Inf	0.0019	-Inf	0.7767
XR_868997.2	3.85	0.0404	-Inf	0.0009	-Inf	0.7840
NR_003364.1	Inf	0.0056	-6.49	0.0071	Inf	1.0000
XR_001779733.1	Inf	0.0003	-6.37	<0.0001	Inf	1.0000
ENSMUST00000174412	Inf	0.0065	-5.51	0.0027	Inf	1.0000
XR_001779736.1	3.55	0.0086	-5.47	0.0001	-1.89	0.6545
ENSMUST00000181532	1.87	0.0151	-5.41	<0.0001	-3.55	0.0283
XR_878681.2	Inf	0.0141	-5.17	0.0112	Inf	1.0000
NR_037998.1	Inf	0.0344	-4.83	0.0201	Inf	1.0000
XR_382352.3	2.63	0.0373	-4.81	0.0002	-2.21	0.4942
NR_045458.1	Inf	0.0175	-4.62	0.0382	Inf	0.9373
XR_388161.1	3.72	0.0464	-4.48	0.0087	-0.77	1.0000
ENSMUST00000131907	6.92	0.0001	-4.38	0.0010	2.55	0.5204
XR_001783822.1	Inf	0.0156	-3.82	0.0254	Inf	0.8663
XR_873120.2	Inf	0.0064	-3.81	0.0343	Inf	0.7787
ENSMUST00000221672	3.83	0.0209	-3.63	0.0179	0.20	1.0000
ENSMUST00000232754	Inf	0.0042	-3.62	0.0109	Inf	0.7343
ENSMUST00000163081	Inf	0.0057	-3.58	0.0370	Inf	0.6962
ENSMUST00000234022	Inf	<0.0001	-3.52	<0.0001	Inf	0.0356
XR_879834.1	4.71	0.0046	-3.16	0.0233	1.54	0.6600
XR_001780251.1	Inf	<0.0001	-3.12	0.0088	Inf	0.0791
XR_390581.3	3.99	0.0096	-2.96	0.0138	1.04	0.7675
TCONS_00007295	2.35	0.0036	-2.92	0.0001	-0.57	0.7765
ENSMUST00000183079	5.47	0.0036	-2.91	0.0464	2.54	0.5123
ENSMUST00000220830	5.04	0.0009	-2.80	0.0083	2.23	0.4355
XR_876739.2	4.94	0.0012	-2.79	0.0226	2.16	0.1841
ENSMUST00000130362	Inf	0.0032	-2.76	0.0331	Inf	0.4430

Table 2 (continued)

Table 2 (continued)

lncRNA_id	Den vs. Ctr		Hi + Den vs. Den		Hi + Den vs. Ctr	
	log2(FC)	P val	log2(FC)	P val	log2(FC)	P val
ENSMUST00000235440	2.18	0.0350	-2.73	0.0029	-0.54	0.6818
ENSMUST00000143649	4.44	<0.0001	-2.72	0.0004	1.71	0.1244
XR_377582.2	5.87	<0.0001	-2.70	0.0007	3.16	0.0173
XR_875669.2	Inf	0.0006	-2.59	0.0205	Inf	0.3736
ENSMUST00000233201	1.69	0.0380	-2.59	0.0017	-0.90	0.3069
XR_869865.2	3.88	0.0014	-2.52	0.0088	1.37	0.4492
XR_382351.2	3.60	0.0055	-2.51	0.0234	1.08	0.5368
XR_877494.2	2.03	0.0113	-2.44	0.0010	-0.41	0.6499
XR_877458.1	4.85	0.0005	-2.44	0.0280	2.43	0.1769
XR_377746.2	Inf	0.0006	-2.42	0.0248	Inf	0.2223
ENSMUST00000197878	Inf	<0.0001	-2.36	0.0033	Inf	0.0020
ENSMUST00000187019	3.28	0.0001	-2.35	0.0010	0.94	0.2181
NR_040268.1	3.26	0.0085	-2.34	0.0156	0.91	0.7053
NR_040290.1	2.89	0.0021	-2.24	0.0062	0.65	0.5297
XR_880009.2	7.76	<0.0001	-2.23	0.0048	5.54	0.0035
NR_045403.1	4.08	0.0011	-2.21	0.0132	1.87	0.3256
TCONS_00005955	6.10	<0.0001	-2.17	0.0084	3.95	0.0025
ENSMUST00000213985	Inf	<0.0001	-2.05	0.0243	Inf	0.0000
XR_384799.3	6.13	0.0002	-2.03	0.0357	4.09	0.0816
TCONS_00017176	3.44	<0.0001	-2.01	0.0035	1.44	0.1079
XR_881514.1	6.56	<0.0001	-1.91	0.0424	4.63	0.1937
NR_015595.3	9.71	<0.0001	-1.89	0.0062	7.82	<0.0001
ENSMUST00000221315	Inf	<0.0001	-1.87	0.0303	Inf	0.0015
XR_001785029.1	3.46	<0.0001	-1.82	0.0057	1.64	0.0124
XR_869015.1	4.75	<0.0001	-1.8	0.0151	2.95	0.0039
ENSMUST00000181427	1.62	0.0394	-1.8	0.0112	-0.18	0.8020
NR_045843.1	2.86	0.0005	-1.77	0.0127	1.09	0.1423
ENSMUST00000133752	4.62	<0.0001	-1.76	0.0301	2.86	0.0240
XR_875986.1	2.45	0.0034	-1.76	0.0156	0.70	0.4005
TCONS_00011293	1.73	0.0267	-1.75	0.0145	-0.02	0.9960
ENSMUST00000226943	2.96	0.0005	-1.73	0.0197	1.23	0.1295
TCONS_00013504	Inf	<0.0001	-1.71	0.0333	Inf	0.0008
NR_027896.1	2.21	0.0039	-1.71	0.0126	0.50	0.4558
TCONS_00012110	3.39	0.0002	-1.71	0.0200	1.69	0.0611

Table 2 (continued)

Table 2 (continued)

lncRNA_id	Den vs. Ctr		Hi + Den vs. Den		Hi + Den vs. Ctr	
	log2(FC)	P val	log2(FC)	P val	log2(FC)	P val
ENSMUST00000185272	1.94	0.0092	-1.67	0.0124	0.28	0.6826
ENSMUST00000133548	8.84	<0.0001	-1.65	0.0174	7.20	0.0000
ENSMUST00000132294	1.78	0.0326	-1.61	0.0343	0.16	0.8344
TCONS_00024432	4.61	<0.0001	-1.59	0.0291	3.02	0.0010
ENSMUST00000149601	2.51	0.0017	-1.56	0.0269	0.95	0.1993
NR_045495.1	3.07	0.0002	-1.55	0.0252	1.52	0.0452
ENSMUST00000236871	2.54	0.0010	-1.54	0.0226	1.00	0.1360
XR_874798.2	2.44	0.0041	-1.54	0.0318	0.91	0.4564
ENSMUST00000142076	8.21	<0.0001	-1.53	0.0401	6.67	<0.0001
TCONS_00027579	2.00	0.0143	-1.53	0.0333	0.48	0.5453
TCONS_00027611	2.00	0.0143	-1.53	0.0333	0.48	0.5453
ENSMUST00000223732	8.00	<0.0001	-1.52	0.0260	6.49	<0.0001
TCONS_00024358	Inf	<0.0001	-1.49	0.0456	Inf	<0.0001
TCONS_00019824	2.06	0.0057	-1.48	0.0249	0.58	0.3726
ENSMUST00000123048	1.83	0.0146	-1.48	0.0275	0.35	0.5991
NR_045904.1	1.85	0.0136	-1.32	0.0486	0.53	0.4232
ENSMUST00000185587	1.55	0.0321	-1.32	0.0445	0.24	0.7013
Upregulated						
ENSMUST00000183180	-Inf	<0.0001	Inf	0.0074	-2.05	0.0341
ENSMUST00000201112	-Inf	<0.0001	Inf	0.0074	-2.05	0.0341
NR_045337.1	-Inf	0.0143	Inf	0.0474	-0.80	0.5951
XR_001778161.1	-Inf	0.0164	Inf	0.0275	-0.56	0.7589
XR_865706.1	-Inf	0.0051	Inf	0.0014	-0.15	0.8675
XR_871930.1	-Inf	0.0059	Inf	0.0001	0.69	0.4889
XR_875613.1	-Inf	0.0042	Inf	0.0268	-1.51	0.2845
XR_879260.1	-Inf	0.0176	Inf	0.0083	-0.04	0.9955
ENSMUST00000191079	-6.46	0.0146	5.27	0.0063	-1.22	0.4296
ENSMUST00000192778	-6.87	<0.0001	5.01	0.0074	-1.86	0.0398
XR_001782817.1	-5.24	0.0245	4.97	0.0049	-0.30	0.8816
TCONS_00019186	-5.79	<0.0001	4.63	0.0121	-1.13	0.1500
ENSMUST00000143847	-5.18	0.0007	4.59	0.0023	-0.57	0.5237
NR_046046.1	-2.96	0.0489	4.44	<0.0001	1.49	0.0955
XR_385889.3	-7.19	<0.0001	4.19	0.0261	-2.98	0.0004

Table 2 (continued)

Table 2 (continued)

lncRNA_id	Den vs. Ctr		Hi + Den vs. Den		Hi + Den vs. Ctr	
	log2(FC)	P val	log2(FC)	P val	log2(FC)	P val
NR_045820.1	-3.74	0.0242	4.17	0.0021	0.44	0.6922
NR_045821.1	-4.31	0.0394	4.14	0.0130	-0.15	0.9607
ENSMUST00000067599	-4.02	0.0179	3.74	0.0111	-0.26	0.8602
ENSMUST00000183245	-2.55	0.0273	3.59	0.0001	1.05	0.1781
ENSMUST00000116345	-3.49	0.0137	3.58	0.0371	0.07	0.9451
NR_040659.1	-4.83	0.0042	3.3	0.0090	-1.50	0.1730
NR_131197.1	-3.44	0.0315	3.27	0.0207	-0.17	0.9143
ENSMUST00000177248	-3.04	0.0481	2.98	0.0288	-0.09	0.9804
XR_877227.1	-2.73	0.0182	2.94	0.0326	0.19	0.7546
ENSMUST00000135378	-3.92	0.0005	2.78	0.0144	-1.15	0.1898
XR_877582.2	-2.27	0.0180	2.39	0.0054	-1.15	0.1898
NR_028422.1	-7.14	0.0002	2.08	0.0457	-5.09	0.0035

FC, fold change; Ctr, control group; Den, denervation group; Hi + Den, HDAC4 inhibition group; lncRNA, long noncoding RNA.

denervation involved in regulation of muscle adaptation, regulation of fatty acid beta-oxidation, and positive regulation of glucose metabolic process, These mRNAs were also found to be involved in several pathways, including autophagy, Ras signaling pathway, FoxO signaling pathway, and Jak-STAT signaling pathway (Figure 4). After HDAC4 inhibition in the ceRNA network that the upregulated lncRNAs belonged to, the mRNAs were found to participate in certain biological processes, including cell cycle and cell division, and in the pathways related to cell cycle (Figure 5).

Key genes in the ceRNA sub-network

In the ceRNA network, hub molecules were identified using MCODE. A total of 19 nodes were selected as hub nodes, including mmu-miR-181c-3p, mmu-miR-181a-1-3p, mmu-miR-3095-3p, mmu-miR-296-5p, Lrrc58, Trim63, Slc39a14, Rras2, Ubxn1, Cat, Sorbs3, Fbxo32, Fam104a, Irs2, Bcl2l1, Mpp6, ENSMUST00000234022, ENSMUST00000143649, and XR_377582.2 (Figure 6). Among them, the number of miRNA-mRNA pairs in miR-3095-3p was the highest, and miR-3095-3p was identified as the core-regulated miRNA. XR_377582.2 and ENSMUST00000143649 bound to the MRE of miR-3095-3p to regulate mRNAs such as Trim63 and Fbxo32,

indicating that these 2 lncRNAs might play a key role in the HDAC4 regulation of denervation-induced skeletal muscle atrophy.

Discussion

In addition to denervation caused by peripheral nerve injury, aging, paralysis, malnutrition, a variety of diseases including cancer, cardiovascular disease, and neurodegenerative diseases can all cause skeletal muscle atrophy (24-27). Reduced protein synthesis and increased protein degradation are the main causes of skeletal muscle atrophy (28). The expression level of HDAC4 has been confirmed to be closely related to various types of muscle atrophy (4,7,29). In previous studies, we discovered and confirmed using mRNA-seq that HDAC4 regulates muscle atrophy by regulating Myog levels and affecting proteolysis (7). In this study, we first performed miRNA-seq, identified 16 upregulated and 16 downregulated miRNAs related to HDAC4-regulated denervation through the comparative analysis, and conducted the KEGG pathway analysis of target genes. Through the comparative analysis of lncRNA-seq, we then identified 111 lncRNAs (27 upregulated and 84 downregulated) related to denervation regulated by HDAC4. Then, we constructed lncRNA-miRNA-mRNA networks related to HDAC4 regulation of muscle atrophy, and conducted GO

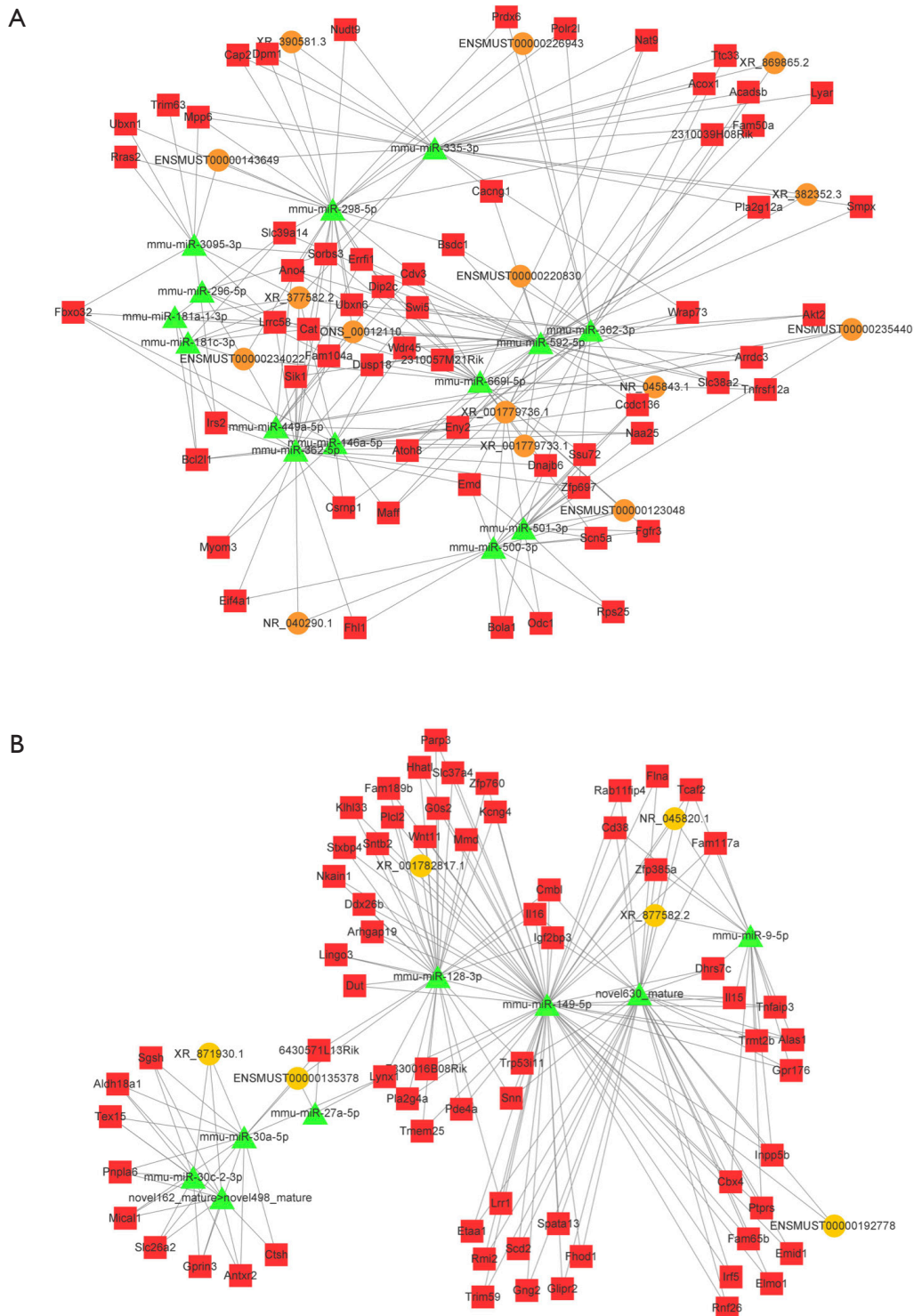


Figure 3 Long noncoding RNA (lncRNA)-related competing endogenous RNA (ceRNA) network regulated by histone deacetylase 4 (HDAC4). (A) The ceRNA network containing downregulated lncRNAs (upregulated lncRNA after denervation and downregulated lncRNA after HDAC4 inhibition), which were screened further. (B) The ceRNA network containing upregulated lncRNAs (downregulated lncRNA after denervation and upregulated lncRNA after HDAC4 inhibition), which were screened further. Triangles represent microRNA (miRNA), squares represent messenger RNA (mRNA), and circles represent lncRNA.

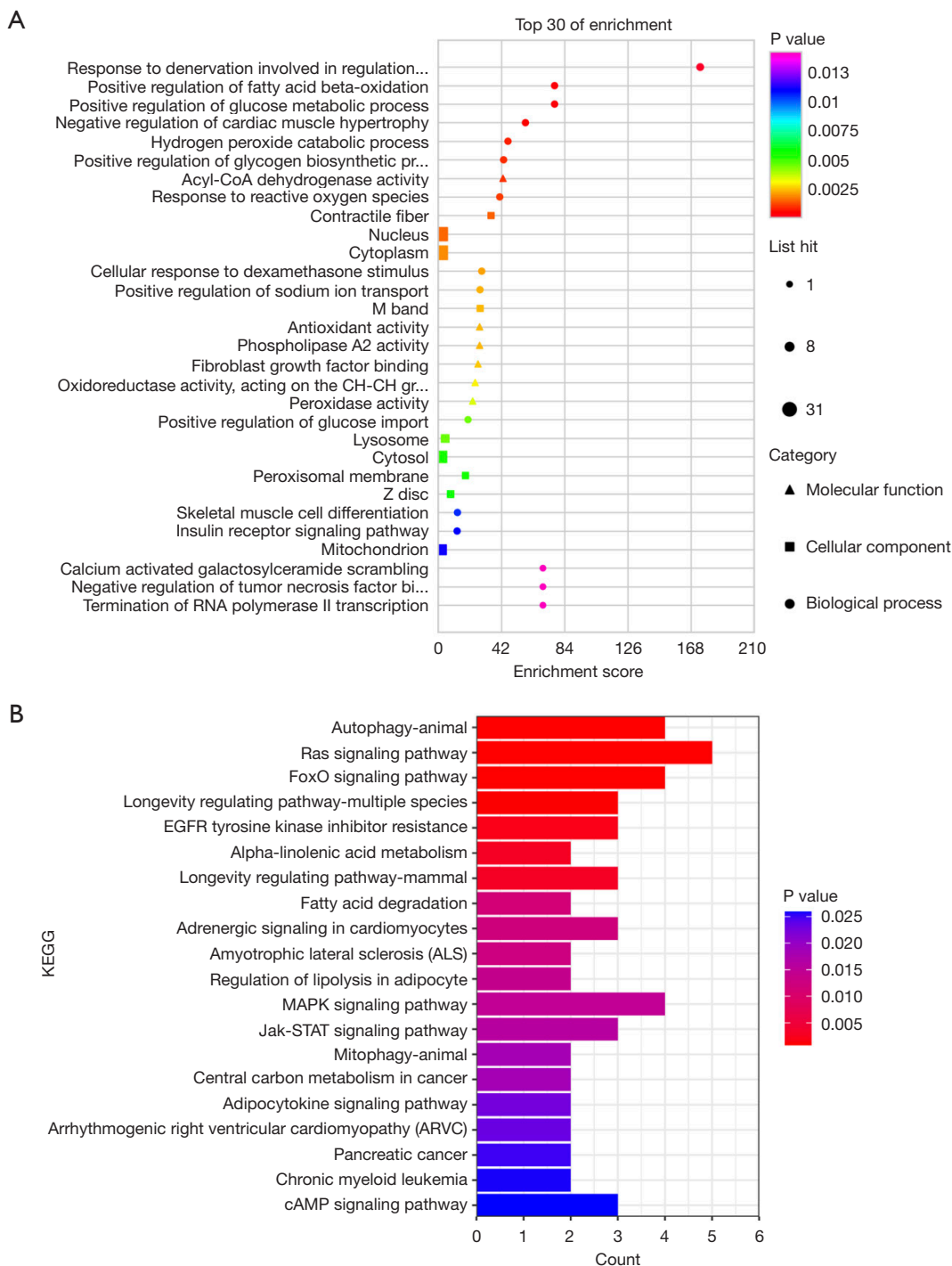


Figure 4 Messenger RNA (mRNA) function enrichment analysis of the competing endogenous RNA (ceRNA) network containing downregulated long noncoding RNA (lncRNAs). (A) The first 30 Gene Ontology (GO) enrichment analysis. The x-axis indicates enriched folds, and the y-axis indicates GO terms. All GO terms are divided into 3 types: triangles represent molecular functions, squares represent cellular components, and circles represent biological processes. The color and size of the bubbles show the P value and number, respectively. (B) The first 20 terms in the Kyoto Encyclopedia of Genes and Genomes (KEGG) pathway enrichment analysis. The x-axis indicates the number of genes, and the y-axis indicates KEGG terms. The bar color indicates the P value.

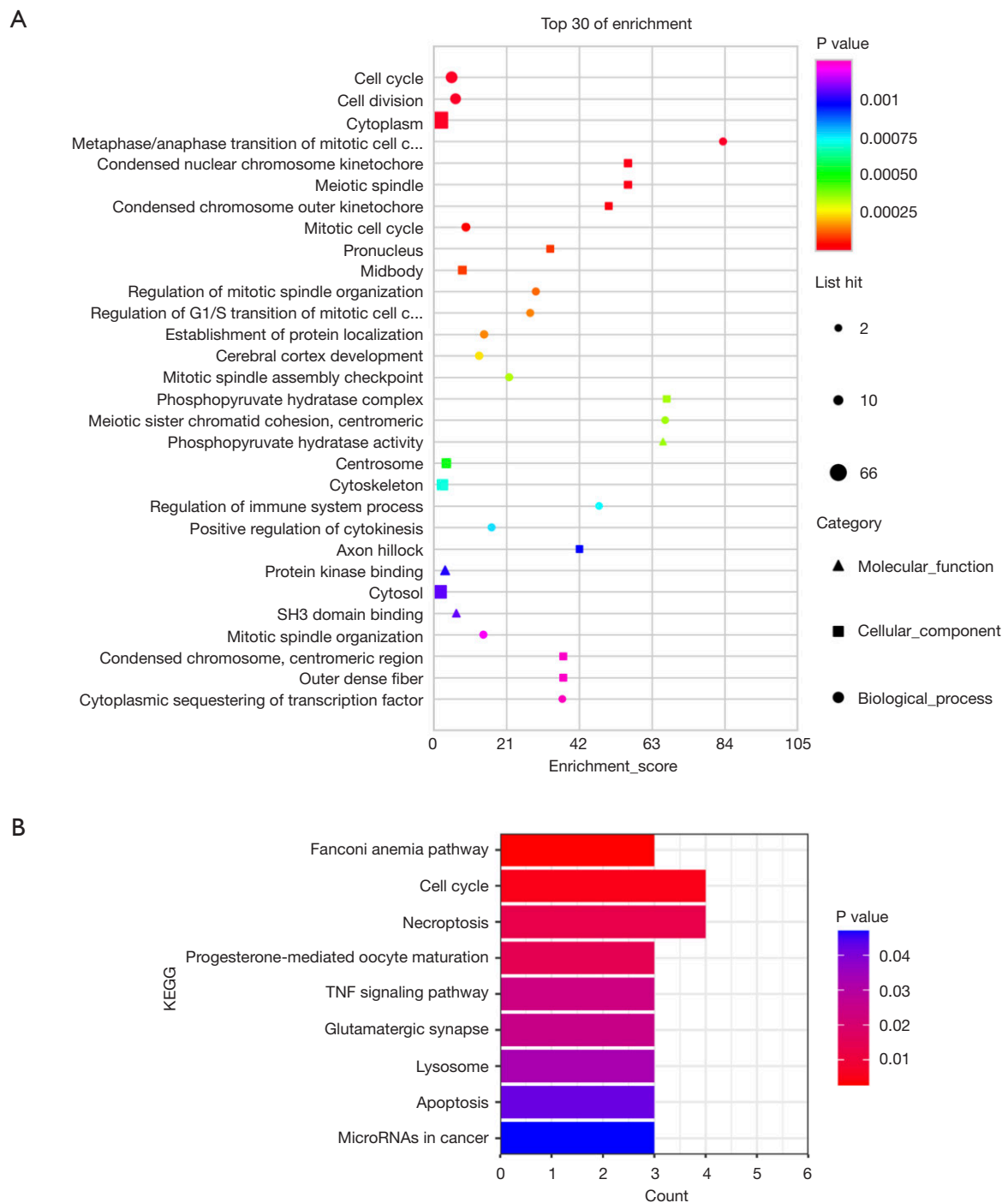


Figure 5 Messenger RNA (mRNA) function enrichment analysis of the competing endogenous RNA (ceRNA) network containing upregulated long noncoding RNA (lncRNAs). (A) The first 30 terms in the Gene Ontology (GO) enrichment analysis. The x-axis indicates enriched folds, and the y-axis indicates GO terms. All GO terms are divided into 3 types: triangles represent molecular functions, squares represent cellular components, and circles represent biological processes. The color and size of the bubbles show the P value and number, respectively. (B) The Kyoto Encyclopedia of Genes and Genomes (KEGG) terms in pathway enrichment analysis. The x-axis indicates the number of genes, and the y-axis indicates KEGG terms. The bar color indicates the P value.

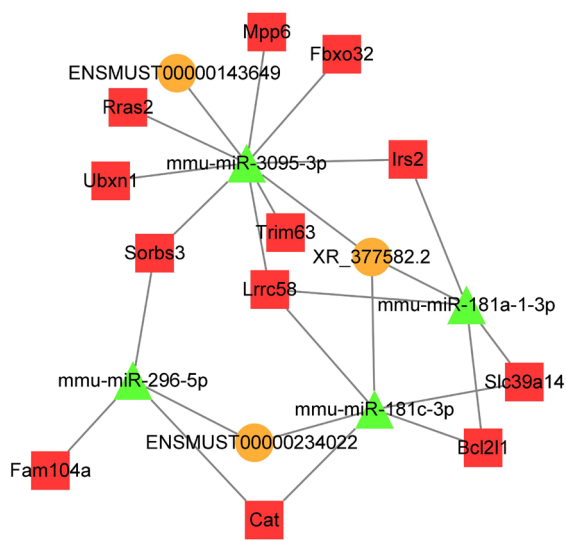


Figure 6 The core subnetwork of long noncoding RNA (lncRNA)-related competing endogenous RNA (ceRNA) network regulated by histone deacetylase 4 (HDAC4). Triangles represent microRNA (miRNA), squares represent messenger RNA (mRNA), and circles represent lncRNA.

function and KEGG pathway enrichment analysis. Finally, we searched for the core regulatory molecules in the ceRNA network in the above lncRNA-miRNA-mRNA network.

Through specific binding to target mRNA, miRNA can accelerate the degradation of target mRNA or inhibit its translation regulatory gene expression. A variety of miRNAs have been reported as being involved in the regulation of skeletal muscle development, differentiation, regeneration, and dysfunction (12,30,31). In this study, we first analyzed the differentially expressed miRNAs related to HDAC4 regulation of muscle atrophy. Muscle-specific miRNAs include miR-1/206 family, miR-133, miR-208, and miR-488. Unfortunately, these muscle-specific miRNAs are not the miRNAs we analyzed here. Nevertheless, KEGG pathway analysis indicated that the target genes of upregulated miRNAs after HDAC4 inhibition were mainly involved in the FoxO signaling pathway and ubiquitin-mediated proteolysis, indicating that miRNAs regulated by HDAC4 are involved in hydrolysis related to muscle atrophy. Target genes of downregulated miRNAs were mainly involved in axon guidance, indicating that miRNAs regulated by HDAC4 are involved in nerve regeneration.

MRE-containing lncRNAs can act as molecular sponges to effectively inhibit miRNA functions. To date, ceRNA

mechanisms and network construction have been mainly investigated in the field of cancer research, and only a few ceRNA interactions have been found to be related to muscle atrophy. Recent research has begun to systematically explore the ceRNA regulatory mechanism for specific muscle atrophies (8,16,25). In this study, we analyzed the differentially expressed lncRNAs related to muscle atrophy regulated by HDAC4. After inhibition of HDAC4, there were 27 upregulated lncRNAs and 84 downregulated lncRNAs. In the ceRNA regulatory network composed of 6 upregulated lncRNAs, 8 downregulated miRNAs, and 66 upregulated mRNAs, the mRNAs were involved in the biological processes and KEGG pathway was mainly related to cell cycle and cell division. For example, E2F transcription factor 1 (E2F1) and RING finger domains 1 (UHRF1) have been found to be closely related to the proliferation of muscle cells (32,33). Furthermore, the proliferation-related genes Forkhead box M1 (*FoxM1*) and Aurora kinase A (*Aurka*) play an important regulatory role in muscle regeneration (34,35). Our previous work showed that HDAC4 may be involved in denervation-induced muscle atrophy by regulating cell division and cell cycle. HDAC4 inhibition reversed the increase of CDKN1A, a cell cycle regulatory protein downstream of p53 gene, in denervated skeletal muscle (7). Here, KEGG analysis showed that the changes in target genes of upregulated miRNAs were associated with mitotically competent cells (“pathways in cancer”, “prostate cancer”, etc.). In the ceRNA network that the upregulated lncRNAs belonged to, the mRNAs participated in cell cycle-related biological processes and pathways. Muscle is a very heterogeneous tissue with many different cell types, and thus how the cell cycle-related genes participated in the HDAC4 regulation of muscle atrophy needs to be determined by further study. In another ceRNA network composed of 15 downregulated lncRNAs, 14 upregulated miRNAs, and 61 downregulated mRNAs, the mRNAs were involved in biological processes such as response to denervation implicated in regulation of muscle adaptation and positive regulation of fatty acid beta-oxidation, as well as pathways such as autophagy, FoxO signaling pathway, and Jak-STAT signaling pathway. In addition to the E3 ubiquitin ligase genes, *FBXO32* and *TRIM63*, the *SCN5A* gene encoding the cardiac sodium channel alpha-subunit (Nav1.5) is involved in the biological processes related to denervation-induced skeletal muscle atrophy. *SCN5A* is usually expressed in neonatal skeletal muscle, which is downregulated rapidly after birth and increased again after denervation-induced

skeletal muscle atrophy (36,37). *Irs2* and *Akt2* are involved in the positive regulation of fatty acid beta-oxidation and glucose metabolic processes. Insulin receptor substrate-1/2 (IRS1/2) is a key protein for insulin and/or insulin growth factor 1 signal transduction. IRS1 plays a leading role in skeletal muscle and is essential for normal myofiber growth and differentiation, insulin-dependent glucose uptake, and glycogen synthesis. As mentioned above, lncIRS1 can regulate the expression of IRS1 through sponging the miR-15 family, thereby alleviating muscle atrophy (16). Although IRS2 and IRS1 are very similar in structural and functional characteristics, they show tissue-specific divergence. The presence of IRS2 in skeletal muscle can be negligible for insulin-induced glucose uptake, and the role of IRS2 in muscle is still unclear (38). Our findings indicate that IRS1 is downregulated after denervation, while IRS2 is upregulated after denervation. Inhibition of HDAC4 can reverse the upregulation of IRS2 caused by denervation. In the models of different glucocorticoid-induced muscle atrophy, there are different changes in IRS2 expression. For instance, high-concentration methylprednisolone can induce an increase in IRS2 expression (39). Therefore, the role of IRS2 in denervation-induced skeletal muscle atrophy regulated by HDAC4 needs to be further explored. *Akt2*-deficient mice have glucose intolerance and present with systemic insulin resistance; however, normal skeletal muscle insulin signals, glucose tolerance, insulin sensitivity, and muscle weight have been detected in skeletal muscle-specific *Akt2*-knockout mice (40). Our previous studies have shown that fatty acid beta oxidation-related genes are generally downregulated 7 days after denervation (1). In this study, we found that β -hydroxy-coenzyme A dehydrogenase (HADH), fatty acid transporter 1 (FATP1/SLC27A1), fatty acid translocase (FAT/CD36), and membrane fatty acid binding protein (FABPpm/GOT2) were all downregulated after denervation. However, inhibition of HDAC4 could not reverse these downregulations caused by denervation. Nonetheless, downregulated miRNA target genes are involved in the regulation of fatty acid biosynthesis. Considering the complexity of miRNA regulatory networks and the expression changes of mRNA mentioned above, we speculated that the mechanism by which HDAC4 controls denervation-induced skeletal muscle atrophy might have little to do with fatty acid β -oxidation (41). In addition, we previously discovered through string analysis that *SIK1*, the key gene which may be involved in HDAC4 regulation of muscle atrophy is also involved in this ceRNA regulatory

network (7). *SIK1* is involved in the regulation of muscle cell differentiation and highly expressed after muscle injury (42).

Finally, we further identified the hub genes in the ceRNA network, including 3 lncRNAs, 4 miRNAs, and 12 mRNAs. In this subnetwork, XR_377582.2 and ENSMUST00000143649 bound to miR-3095-3p and played a core regulatory role by regulating *fbxo32*, *trim63*, *Mpp6*, *Ras2*, *Irs2*, *Ubxn1*, *Sorbs3*, and *Lrrc58*. After HDAC4 inhibition, the level of miR-3095-3p (log₂ FC = 2.89) was significantly upregulated, ranking second among all upregulated miRNAs, while XR_377582.2 (log₂ FC = -2.703) and ENSMUST00000143649 (log₂ FC = -2.723) levels were significantly downregulated. These mRNAs were mainly involved in biological processes, such as responses to denervation involved in regulation of muscle adaptation and cell migration, as well as the FoxO, Ras, and MAPK signaling pathways. The limitations of the network should be acknowledged. Systematic and rigorous experiments are warranted in the future to further verify our findings. Thus far, little has been reported on XR_377582.2, ENSMUST00000143649, and miR-3095-3p. miR-3095 can be found in the mouse version in the miRBase database. Only a few human and mouse lncRNAs are orthologues, and most of the lncRNAs are species-specific. Neither XR_377582.3 nor ENSMUST00000143649 appear to have a human orthologue on ENSEMBL or Blast. Therefore, our findings might be more important from a biological perspective and may provide a theoretical basis for the alleviation of skeletal atrophy by HDAC4.

In conclusion, all nodes in the ceRNA network directly or indirectly participate in the process of HDAC4 regulating denervation-induced skeletal muscle atrophy. XR_377582.2 and ENSMUST00000143649 may be the key lncRNAs related to HDAC4 involved in the regulation of muscle atrophy in mice. Our findings further provide a theoretical basis to explain how HDAC4 acts as a key target for effectively delaying denervation-induced skeletal muscle atrophy.

Acknowledgments

Funding: This work was supported by the Natural Science Foundation of Jiangsu Province (No. BK20201209), the National Natural Science Foundation of China (Grant Nos. 81871554 and 81901933), the QingLan Project at Jiangsu Universities, and the Priority Academic Program Development of Jiangsu Higher Education Institutions.

Footnote

Reporting Checklist: The authors have completed the ARRIVE reporting checklist. Available at <https://atm.amegroupp.com/article/view/10.21037/atm-21-6512/rc>

Data Sharing Statement: Available at <https://atm.amegroupp.com/article/view/10.21037/atm-21-6512/dss>

Conflicts of Interest: All authors have completed the ICMJE uniform disclosure form (available at <https://atm.amegroupp.com/article/view/10.21037/atm-21-6512/coif>). The authors have no conflicts of interest to declare.

Ethical Statement: The authors are accountable for all aspects of the work in ensuring that questions related to the accuracy or integrity of any part of the work are appropriately investigated and resolved. Experiments were performed under a project license (No. 20180305-004) granted by the Jiangsu Laboratory Animal Management Committee, in compliance with the Nantong University guidelines for the care and use of animals.

Open Access Statement: This is an Open Access article distributed in accordance with the Creative Commons Attribution-NonCommercial-NoDerivs 4.0 International License (CC BY-NC-ND 4.0), which permits the non-commercial replication and distribution of the article with the strict proviso that no changes or edits are made and the original work is properly cited (including links to both the formal publication through the relevant DOI and the license). See: <https://creativecommons.org/licenses/by-nc-nd/4.0/>.

References

- Shen Y, Zhang R, Xu L, et al. Microarray Analysis of Gene Expression Provides New Insights Into Denervation-Induced Skeletal Muscle Atrophy. *Front Physiol* 2019;10:1298.
- Gordon T. Peripheral Nerve Regeneration and Muscle Reinnervation. *Int J Mol Sci* 2020;21:8652.
- Gu X, Ding F, Yang Y, et al. Construction of tissue engineered nerve grafts and their application in peripheral nerve regeneration. *Prog Neurobiol* 2011;93:204-30.
- Luo L, Martin SC, Parkington J, et al. HDAC4 Controls Muscle Homeostasis through Deacetylation of Myosin Heavy Chain, PGC-1 α , and Hsc70. *Cell Rep* 2019;29:749-763.e12.
- Yoshihara T, Tsuzuki T, Chang SW, et al. Exercise preconditioning attenuates hind limb unloading-induced gastrocnemius muscle atrophy possibly via the HDAC4/Gadd45 axis in old rats. *Exp Gerontol* 2019;122:34-41.
- Mochalova EP, Belova SP, Kostrominova TY, et al. Differences in the Role of HDACs 4 and 5 in the Modulation of Processes Regulating MAFbx and MuRF1 Expression during Muscle Unloading. *Int J Mol Sci* 2020;21:4815.
- Ma W, Cai Y, Shen Y, et al. HDAC4 Knockdown Alleviates Denervation-Induced Muscle Atrophy by Inhibiting Myogenin-Dependent AtroGene Activation. *Front Cell Neurosci* 2021;15:663384.
- Yue B, Li H, Liu M, et al. Characterization of lncRNA-miRNA-mRNA Network to Reveal Potential Functional ceRNAs in Bovine Skeletal Muscle. *Front Genet* 2019;10:91.
- Hitachi K, Nakatani M, Funasaki S, et al. Expression Levels of Long Non-Coding RNAs Change in Models of Altered Muscle Activity and Muscle Mass. *Int J Mol Sci* 2020;21:1628.
- Wada S, Kato Y, Okutsu M, et al. Translational suppression of atrophic regulators by microRNA-23a integrates resistance to skeletal muscle atrophy. *J Biol Chem* 2011;286:38456-65.
- Kukreti H, Amuthavalli K, Harikumar A, et al. Muscle-specific microRNA1 (miR1) targets heat shock protein 70 (HSP70) during dexamethasone-mediated atrophy. *J Biol Chem* 2013;288:6663-78.
- Qiu J, Zhu J, Zhang R, et al. miR-125b-5p targeting TRAF6 relieves skeletal muscle atrophy induced by fasting or denervation. *Ann Transl Med* 2019;7:456.
- Qiu J, Wang L, Wang Y, et al. MicroRNA351 targeting TRAF6 alleviates dexamethasone-induced myotube atrophy. *J Thorac Dis* 2018;10:6238-46.
- Salmena L, Poliseno L, Tay Y, et al. A ceRNA hypothesis: the Rosetta Stone of a hidden RNA language? *Cell* 2011;146:353-8.
- Cesana M, Cacchiarelli D, Legnini I, et al. A long noncoding RNA controls muscle differentiation by functioning as a competing endogenous RNA. *Cell* 2011;147:358-69.
- Li Z, Cai B, Abdalla BA, et al. LncIRS1 controls muscle atrophy via sponging miR-15 family to activate IGF1-PI3K/AKT pathway. *J Cachexia Sarcopenia Muscle* 2019;10:391-410.
- Qiu J, Fang Q, Xu T, et al. Mechanistic Role of Reactive Oxygen Species and Therapeutic Potential of Antioxidants

- in Denervation- or Fasting-Induced Skeletal Muscle Atrophy. *Front Physiol* 2018;9:215.
18. Wang W, Shen D, Zhang L, et al. SKP-SC-EVs Mitigate Denervated Muscle Atrophy by Inhibiting Oxidative Stress and Inflammation and Improving Microcirculation. *Antioxidants (Basel)* 2021;11:66.
 19. Cui Q, Yang H, Gu Y, et al. RNA sequencing (RNA-seq) analysis of gene expression provides new insights into hindlimb unloading-induced skeletal muscle atrophy. *Ann Transl Med* 2020;8:1595.
 20. Langmead B, Salzberg SL. Fast gapped-read alignment with Bowtie 2. *Nat Methods* 2012;9:357-9.
 21. Zhao Y, Lin Q, Li N, et al. MicroRNAs profiles of Chinese Perch Brain (CPB) cells infected with *Siniperca chuatsi rhabdovirus (SCRV)*. *Fish Shellfish Immunol* 2019;84:1075-82.
 22. Tay Y, Kats L, Salmena L, et al. Coding-independent regulation of the tumor suppressor PTEN by competing endogenous mRNAs. *Cell* 2011;147:344-57.
 23. Wu G, Wan X, Xu B. A new estimation of protein-level false discovery rate. *BMC Genomics* 2018;19:567.
 24. Madaro L, Passafaro M, Sala D, et al. Denervation-activated STAT3-IL-6 signalling in fibro-adipogenic progenitors promotes myofibres atrophy and fibrosis. *Nat Cell Biol* 2018;20:917-27.
 25. Hitachi K, Nakatani M, Kiyofuji Y, et al. An Analysis of Differentially Expressed Coding and Long Non-Coding RNAs in Multiple Models of Skeletal Muscle Atrophy. *Int J Mol Sci* 2021;22:2558.
 26. Sartori R, Romanello V, Sandri M. Mechanisms of muscle atrophy and hypertrophy: implications in health and disease. *Nat Commun* 2021;12:330.
 27. Yang X, Ji Y, Wang W, et al. Amyotrophic Lateral Sclerosis: Molecular Mechanisms, Biomarkers, and Therapeutic Strategies. *Antioxidants (Basel)* 2021;10:1012.
 28. Bonaldo P, Sandri M. Cellular and molecular mechanisms of muscle atrophy. *Dis Model Mech* 2013;6:25-39.
 29. Moresi V, Williams AH, Meadows E, et al. Myogenin and class II HDACs control neurogenic muscle atrophy by inducing E3 ubiquitin ligases. *Cell* 2010;143:35-45.
 30. Horak M, Novak J, Bienertova-Vasku J. Muscle-specific microRNAs in skeletal muscle development. *Dev Biol* 2016;410:1-13.
 31. Huang QK, Qiao HY, Fu MH, et al. MiR-206 Attenuates Denervation-Induced Skeletal Muscle Atrophy in Rats Through Regulation of Satellite Cell Differentiation via TGF- β 1, Smad3, and HDAC4 Signaling. *Med Sci Monit* 2016;22:1161-70.
 32. Luo W, Li G, Yi Z, et al. E2F1-miR-20a-5p/20b-5p auto-regulatory feedback loop involved in myoblast proliferation and differentiation. *Sci Rep* 2016;6:27904.
 33. Zheng TF, Liu XL, Li X, et al. Dickkopf-1 promotes Vascular Smooth Muscle Cell proliferation and migration through upregulating UHRF1 during Cyclic Stretch application. *Int J Biol Sci* 2021;17:1234-49.
 34. Wang YX, Feige P, Brun CE, et al. EGFR-Aurka Signaling Rescues Polarity and Regeneration Defects in Dystrophin-Deficient Muscle Stem Cells by Increasing Asymmetric Divisions. *Cell Stem Cell* 2019;24:419-432.e6.
 35. Chen Z, Li L, Xu S, et al. A Cdh1-FoxM1-Apc axis controls muscle development and regeneration. *Cell Death Dis* 2020;11:180.
 36. Carreras D, Martinez-Moreno R, Pinsach-Abuin ML, et al. Epigenetic Changes Governing Scn5a Expression in Denervated Skeletal Muscle. *Int J Mol Sci* 2021;22:2755.
 37. Hendrickse P, Galinska M, Hodson-Tole E, et al. An evaluation of common markers of muscle denervation in denervated young-adult and old rat gastrocnemius muscle. *Exp Gerontol* 2018;106:159-64.
 38. Eckstein SS, Weigert C, Lehmann R. Divergent Roles of IRS (Insulin Receptor Substrate) 1 and 2 in Liver and Skeletal Muscle. *Curr Med Chem* 2017;24:1827-52.
 39. Fappi A, Neves JC, Sanches LN, et al. Skeletal Muscle Response to Deflazacort, Dexamethasone and Methylprednisolone. *Cells* 2019;8:406.
 40. Jaiswal N, Gavin MG, Quinn WJ 3rd, et al. The role of skeletal muscle Akt in the regulation of muscle mass and glucose homeostasis. *Mol Metab* 2019;28:1-13.
 41. Fritzen AM, Lundsgaard AM, Kiens B. Tuning fatty acid oxidation in skeletal muscle with dietary fat and exercise. *Nat Rev Endocrinol* 2020;16:683-96.
 42. Stewart R, Akhmedov D, Robb C, et al. Regulation of SIK1 abundance and stability is critical for myogenesis. *Proc Natl Acad Sci U S A* 2013;110:117-22.
- (English Language Editors: B. Meiser and J. Gray)

Cite this article as: Gu Y, Lin Y, Li M, Zong C, Sun H, Shen Y, Zhu J. An analysis of lncRNA-miRNA-mRNA networks to investigate the effects of HDAC4 inhibition on skeletal muscle atrophy caused by peripheral nerve injury. *Ann Transl Med* 2022;10(9):516. doi: 10.21037/atm-21-6512